

OPTIMIZATION OF MAGNETIC LENSES FOR WAVEGUIDE PORTION OF A PROTON LINAC\*

William M. Visscher, University of California  
 Los Alamos Scientific Laboratory  
 Los Alamos, New Mexico

Summary

A discussion of factors affecting the radial confinement of the beam in a waveguide proton linac is given. Simple analytic expressions are developed which check with computer results. Consideration of radial acceptance, tolerance to errors, cost, length, and complexity, seems to indicate that doublet magnetic lenses are preferable to triplets.

Introduction

The function of the quadrupole magnets in a linac is to confine the beam; to counteract the radially expansive effects of the RF fields and alignment errors. The magnet system parameters are therefore inseparable from many other accelerator parameters, and any discussion of optimization of the lenses involves consideration of all the electromagnetic fields which determine the particle orbits. Before asking about the magnet systems, therefore, we must to some extent specify the RF and geometrical features of the linac.

In the following, we shall state these boundary conditions and set up a simple mathematical model for the linac. Limits on certain accelerator parameters may be derived approximately and written in simple algebraic forms. Similarly, the gross effects of errors of various sorts in component alignment, field phases and amplitudes may be transparently exhibited.

The importance of these rough formulae stems from their simplicity and from the fact that they are in substantial agreement with the results of an accurate computer calculation. They facilitate an uncomplicated but quantitative understanding of the relations between linac parameters.

Boundary Conditions

A minimization of RF power plus fabrication costs dictates that the energy gain per meter be nearly constant throughout the waveguide linac. The relative shunt impedances of  $2\pi$  and  $\pi$ -mode structures as well as beam quality and acceptance are factors in the determination of the initial energy. Constraints are imposed on tank lengths by the desirability of uniformity in power supplies and the constancy of the RF gradient. Figure 1 shows the relation imposed between synchronous energy and number of  $\pi$ -mode cells per section by the requirements that a) the synchronous particle gains 1.3 Mev/meter, b) the power consumption in the section be 1, 1/2, or 1/4 Mw. Cloverleaf shunt impedances<sup>2</sup> and a 20 ma beam current are assumed. Plotted also on Fig. 1 is an upper limit on  $n_c$  derived below.

Phase and radial qualities of the input beam are still in doubt. Because of the frequency jump from 200 Mc in the drift tube section to 800 Mc the phase spread is quadrupled at the transition; to make the beam loss tolerable the waveguide phase acceptance must be nearly 90°. Radial acceptance is less critical; both kinds are determined by computer.

Model Accelerator

The geometrical parameters of our linac model are defined in Fig. 2. The RF parameters are fixed by taking the fields to be those of the  $TM_{01}$  mode in a circular waveguide with the guide wavelength equal to 2 cell lengths. The equivalence of these fields to the actual cavity fields can be established for the energies which interest us.<sup>3</sup>

The longitudinal and radial impulses received by a proton moving parallel to the axis at constant speed through one cell are

$$I_z = \frac{\pi E_0}{2\omega} I_0(\kappa r) \cos \phi \quad (1)$$

$$I_r = -\frac{\pi E_0}{2\omega \gamma} I_1(\kappa r) \sin \phi,$$

where  $E_0$  is the peak field on the axis,  $\kappa = \pi/L$  ( $L =$  cell length  $= \beta\lambda/2$ ),  $\phi$  is the phase of the particle relative to the RF crest, and the  $I$ 's are the Bessel functions of imaginary argument. Equation (1) makes explicit the relation between the accelerating field and the defocussing field. The impulse approximation implied therein is quite accurate for our energies.

The transverse deflection suffered by a particle passing through a quadrupole lens is calculated by standard means:

$$\begin{bmatrix} x' \\ v_x' \end{bmatrix} = \begin{bmatrix} \cos \Omega t & \frac{1}{\Omega} \sin \Omega t \\ -\Omega \sin \Omega t & \cos \Omega t \end{bmatrix} \begin{bmatrix} x \\ v_x \end{bmatrix} \quad (2)$$

for a converging quad; for a diverging one  $\Omega$  is replaced by  $i\Omega$ .  $\Omega$  is the natural transverse oscillation frequency of the particle orbit. For protons

$$(\Omega/\omega)^2 = 3.22(\lambda/2\pi)^2 \frac{B}{\gamma} \text{H' (Kilogauss/cm)}, \quad (3)$$

where  $\lambda$  is in meters. Our computer code, which is described elsewhere,<sup>3</sup> uses Eqs. (1) and (2) and other equations accounting for drift spaces and errors to transport bunches of particles through the model accelerator of several thousand cells.

Analytic Approximations

It is desirable to have some sort of analytic handle on parameter variation to reduce the amount of numerical experimentation needed. To this end we consider the following crude picture of the particle orbits. On Fig. 2 are drawn two particle orbits, one never crossing the  $xz$  plane and the other crossing it every section. It is intuitively obvious that these represent the lower limit of magnetic lens strength for a stable orbit (focussing force just sufficient to counteract the defocussing) and the upper limit (any increase in focussing can only increase the amplitude) respectively.<sup>4</sup> If these orbits are approximated with straight line segments in the accelerator section and the effect of the magnetic lenses calculated to lowest order in magnetic field gradient, and if  $Q = H'^2 d_m^2 (D - 2/3 D_m)$ , (wherein  $H'$  is in

kilogauss/cm, other distances are all in meters,  $D_m = 2d_m$  for doublets,  $4d_m$  for triplets), the limits are

$$Q > -0.152 \frac{n_c}{\gamma} \frac{W \tan \varphi_s}{mc^2}, \quad (4a)$$

$$Q < -0.076 \frac{n_c}{\gamma} \frac{W \tan \varphi_s}{mc^2} + 0.772 \frac{\gamma^2 \beta}{n_c \lambda}, \quad (4b)$$

where  $W$  is the energy gain per meter and the orbit is synchronous with  $\varphi = \varphi_s < 0$ .

If one now takes the further step of assuming that the radial wavelength contains many sections and that the change in radius in any section is small compared to the radial amplitude, then an approximate equation for the radial motion is

$$\frac{d^2 r}{dt^2} + \frac{\dot{\gamma}}{\gamma} \frac{dr}{dt} + \Omega_r^2 r = 0, \quad (5)$$

$$\Omega_r^2 = \frac{\omega \Omega^2 (\Omega t)^2 (T - \frac{2}{3} T_m)}{n_c^2} + \frac{\omega c}{\beta \gamma^3} \frac{W \sin \varphi}{mc^2 \cos \varphi_s} \quad (6)$$

which is the radial oscillation frequency. The dependent variable in Eq. (5) should actually be  $x$  or  $y$ . We ignore the distinction and also prohibit azimuthal motion.  $T$  and  $T_m$  are  $D$  and  $D_m/\beta c$ ; we note that

$$\Omega^2 (\Omega t)^2 (T - \frac{2}{3} T_m) = \frac{10.36c}{\gamma \beta} Q. \quad (7)$$

A similar equation for the phase motion is, after linearizing in  $(\varphi - \varphi_s) = \tilde{\varphi}$

$$\frac{d^2 \tilde{\varphi}}{dt^2} + \frac{d \log \beta^2 \gamma^3}{dt} \frac{d\tilde{\varphi}}{dt} + \Omega_\varphi^2 \tilde{\varphi} = 0, \quad (8)$$

with

$$\Omega_\varphi^2 = -\frac{\omega c}{\beta \gamma^3} \frac{W \tan \varphi_s}{mc^2} I_0(\kappa r). \quad (9)$$

Equations (5) and (8) contain radial-phase coupling terms exhibited in Eqs. (6) and (9). A simultaneous solution shows the effects of the radial-phase resonances, exemplified in a computer calculation on Fig. 3. For now we ignore the interaction and set  $I_0 = 1$  in Eq. (9) and  $\varphi = \varphi_s$  in Eq. (6). Then putting  $\Omega_\varphi^2 = \Omega_r^2$  yields the condition for radial-phase resonance,

$$\Omega^2 (\Omega t)^2 (T - \frac{2}{3} T_m) = -\frac{3}{2} \frac{n_c \pi c}{\gamma^3 \beta} \frac{W \tan \varphi_s}{mc^2}. \quad (10)$$

If the  $3/2$  here is replaced by  $1/2$ , Eq. (10) becomes identical to the condition for  $\Omega_r^2 = 0$  (Eq. 4a).

There is a limit on the length of the accelerator sections which is independent of the focussing systems. Namely, the length in which an input bunch of protons of a given radial quality will be expanded so far that it begins to exceed the aperture at the end of the section. This gives a relation between aperture, RF amplitude and phase, beam quality, energy, and section length which can be easily derived but whose

usefulness is impaired by its complexity. Simpler and fortuitously accurate in practice is the condition that a proton going into the section in an exponential orbit will have its radius e-folded coming out. This is

$$n_c^2 < -\frac{4\gamma^3 \beta}{\pi \lambda} \frac{mc^2}{W \tan \varphi_s}. \quad (11)$$

Equations (4) and (11) are plotted on Fig. 4 which gives boundaries of the stable regions in  $n_c, Q$  for several energies. The source of our confidence in the qualitative correctness of these considerations is that the numerical results for the limits of  $Q$  agree to  $\approx 20\%$  with these, and Eq. (11) is quite accurate too for values of  $Q$  about 2 or 3 times the minimum. Previous computer results<sup>3</sup> indicated that Eq. (10), not Eq. (4a), should define the lower limit for lens strength. We still believe this to be true in the neighborhood of the maximum value of  $n_c$ . When the radial and phase oscillation are resonant, for some orbits  $-\varphi$  will be large when  $r$  is and the effective defocussing larger than implied by  $\varphi_s$ . For these orbits Eq. (11) puts a smaller limit on  $n_c$ . Thus the lower corners in Fig. 4 should be rounded (as should the upper ones by an equally evident mechanism). Figure 3 shows computer examples of orbits near the upper and lower limits of  $Q$ .

Plotted on Fig. 1 is Eq. (11). It dictates that the section length be on the  $1/4$  Mw curve to start, jumping up at two transition energies to give a composite like that illustrated. The sudden changes in section length seem to generate only minor beam-dynamical problems.

It is desirable that an unpowered beam, either coasting or out of the phase bucket, seeing incoherent RF, be radially stable. The condition for this is

$$Q < 0.772 \frac{\gamma^2 \beta^2}{n_c \lambda \beta_s} \quad (12)$$

which is plotted on Fig. 4 too.

#### RF Errors

If  $\beta$  is considered to change adiabatically, Eq. (8) can be integrated to give

$$\tilde{\varphi}(t) = S(t, t') \tilde{\varphi}(t') \quad (13a)$$

$$S(t, t') = [(\beta \gamma)_{t'} / (\beta \gamma)_t]^{3/4} e^{i \int_{t'}^t \Omega_\varphi(t'') dt''} \quad (13b)$$

If one assumes that at a set of times  $t_\kappa$  ( $\kappa = 1, N$ ) independent random phase displacements are introduced, the increase in the mean square phase spread will be approximately

$$\Delta < \tilde{\varphi}(t)^2 > = \sum_{\kappa=1}^N [(\beta \gamma)_{t_\kappa} / (\beta \gamma)_t]^{3/4} \delta \varphi_\kappa^2, \quad (14)$$

which exhibits the phase damping factor.

Independent random errors in RF amplitude or phase effectively cause random jumps in  $\tilde{\varphi}$  and give an increase in mean square phase spread of roughly

$$\Delta < \tilde{\varphi}(t)^2 > = (\beta \gamma)_t^{-3/2} \frac{W \cot \varphi_s}{mc^2} \frac{\pi \lambda n_c^2}{2} \times$$

$$\times \sum_K \left( \frac{\beta}{\gamma} \right)_K^{\frac{1}{2}} \left( \frac{\delta W_K}{W} \right)^2 \quad (15)$$

where  $\delta W_K/W$  is the fractional error in energy gain in the  $K$ th section due either to an RF phase or amplitude error. This underlines the fact that RF errors are amplified for long sections, high fields, low energies, and low frequencies.

Equations (14) and (15) are in agreement within a factor of 2 with appropriate computer results.

Alignment Errors

In the same way, an adiabatic integration of Eq. (5) yields the approximate solution

$$r(t) = T(t, t') r(t') \quad (16a)$$

$$T(t, t') = [(\gamma \Omega_r)_t]^{\frac{1}{2}} / [(\gamma \Omega_r)_{t'}]^{\frac{1}{2}} e^{i \int_{t'}^t \Omega_r(t'') dt''} \quad (16b)$$

This can be used to produce approximations to the radial spread caused by various kinds of errors in alignment of magnets and tanks.

Random jumps in  $r$  due to uncorrelated section misalignments, for example, give an increase in mean squared radial spread of

$$\Delta < r(t)^2 > = \sum_K \delta r_K^2 (\gamma \Omega_r)_K / (\gamma \Omega_r)_t \quad (17)$$

in which the second factor may or may not be a damping factor depending on how the magnet gradients are programmed [see Eq. (6)].

If the magnet systems as units suffer random transverse displacements  $\delta R_K$  then the particle will receive impulses proportional to  $Q \delta R_K$  which will, by application of Eqs. (16) cause an increase in radial spread of about

$$\Delta < r(t)^2 > = \sum_K \delta R_K^2 \times \left( \frac{\gamma}{\Omega_r} \right)_K \frac{(\Omega_r^2 + \frac{1}{2} \Omega_\phi^2)_K}{(\gamma \Omega_r)_t} (2\pi L_s)^2 \left( \frac{1}{\lambda_r^2} + \frac{1}{2\lambda_\phi^2} \right) \quad (18)$$

where  $L_s$  is the section length and  $\lambda_r, \lambda_\phi$  are the radial and phase oscillation wavelengths. This equation says that the seriousness of transverse lens misalignments increases for short radial wavelengths (strong lenses), but that for  $\lambda_r \approx 2\pi L_s$  (usually approximately realized in practice) these tolerances are no more stringent than those on section misalignments [Eq. (17)].

Very similar in form to Eq. (18) is the spread increase due to random displacements of the individual magnets.

$$\Delta < r(t)^2 > = \sum_K \delta R_K^2 \left( \frac{\gamma}{\Omega_r} \right)_K \frac{(\Omega_r^2 + \frac{1}{2} \Omega_\phi^2)_K}{(\gamma \Omega_r)_t} Z_K \frac{L_s}{D - \frac{2}{3} D_m} \quad (19)$$

in which  $Z_K = 4$  for the center magnet of a triplet, unity otherwise. Equation (19) exhibits an amplification factor for individual magnet errors of the order of the ratio of the section length to the effective lens drift length.

Rotations of the magnet systems about a transverse axis are serious for doublets (being equivalent to individual transverse displacements with pairwise constructive correlations), not serious for triplets (individual correlations are destructive, net effect comparable to transverse displacement of system).

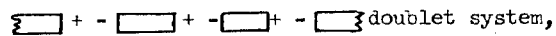
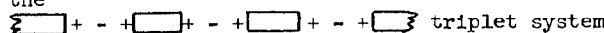
Rotations of the individual magnets about the longitudinal axis are equivalent to transverse displacements of the individual magnets with  $r \sin \delta \phi$  replacing  $\delta R_K$  where  $r$  is the orbit radius and  $\delta \phi$  the rotation angle.

Where comparisons with computer runs have been made, the foregoing formulae and statements about errors have been semi-quantitatively (factor of two or better) verified. The dramatic difference in sensitivity to individual magnet errors and to errors in system positions in particular is well verified.<sup>5</sup>

Radial Acceptance

Some significant differences between the triplet and doublet systems are higher cost, length, and power consumption for triplet and more difficult transverse alignment for doublets. Radial acceptance will be decisive if it is significantly different for the two cases. Radial-phase coupling drastically affects the acceptance hyperfish because its boundaries in 6-dimensional phase space are far in the nonlinear domain. Most reliable information about acceptance is therefore dependent on computer results.

Some such results are shown in Fig. 5a where radial acceptances are shown for a monoenergetic 50 Mev bunch with a 90° phase spread. Figure 5b shows how the population of such a bunch (transverse quality  $\approx 15 \pi$  mr-cm) is depleted going from 50 to 800 Mev. All these calculations are for the

 doublet system, and the  triplet system.

Considerable numerical experimentation has been performed with other sequences, but these seem to be best.

Random 2 mil individual transverse displacements of the quad magnets does not materially reduce the acceptance for either doublets or triplets. Both systems show effects of 4 mil errors. Because the triplets, in contrast to the doublets, can be bench aligned, these tolerances are more serious for the doublets, but are not excessively stringent. Longitudinal rotation tolerances of the quads are tighter for triplets than for doublets, about 1/2 and 1 degree, respectively.

\* This work was performed under the auspices of the U. S. Atomic Energy Commission.

References

1. D. E. Nagle (unpublished).
2. E. A. Knapp, Proceedings of 1964 MURA Linear Accelerator Conference.
3. M. Jakobson and W. M. Visscher, Proceedings of the 1964 MURA Linear Accelerator Conference and unpublished work.
4. They correspond to the cases for  $\cos\mu = \pm 1$  of L. Smith and R. L. Gluckstern (Rev. Sci.Inst. 26 220 (1955)).
5. That this should be the case was elegantly shown by Gluckstern (Yale Internal Report Y-7).

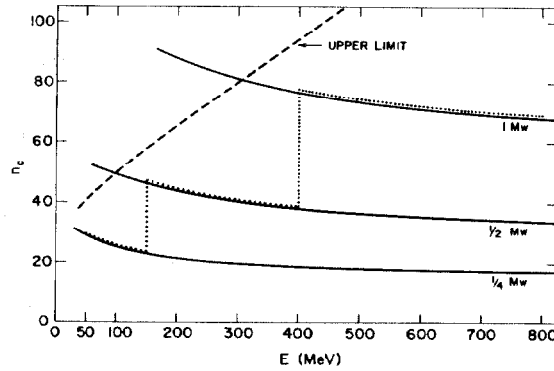


Fig. 1. Solid curves are the numbers of  $\pi$ -mode cells per section for the indicated power consumption. Measured shunt impedances (E. Knapp, private communication) for cloverleaf cavities, a constant RF gradient of 1.3 Mev per meter energy gain, and a beam current of 20 ma are assumed. Dashed curve is an analytic approximation to the beam-dynamical upper limit. Dotted curve is the resultant optimum section length as a function of energy for a 50  $\rightarrow$  800 Mev waveguide type proton linac.

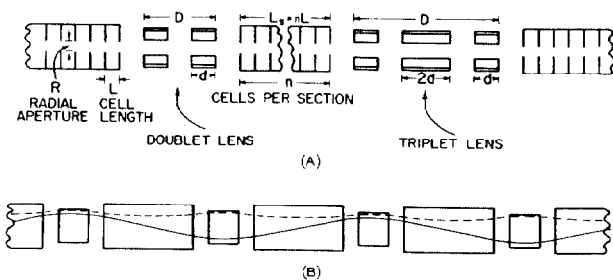


Fig. 2. (a) Geometrical parameters for accelerator tanks and magnet systems. (b) Dashed line represents particle orbit for minimum strength lenses, solid line for maximum.

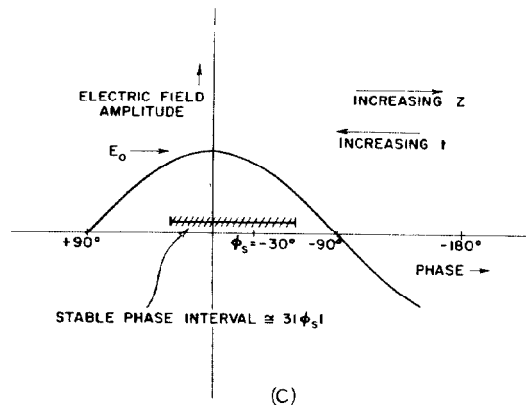


Fig. 2. (c) RF phase convention. Energy gain/meter =  $W = 1/2 E_0 \cos \phi$ . Transit time factor is identically 1/2 for our assumed simple geometry.

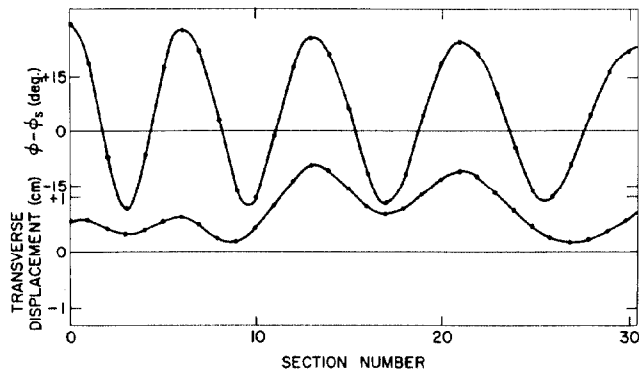


Fig. 3(a). Computer results for orbit radius and phase for minimum lens strength ( $\lambda_L = \infty$ ; Eq. (4a)). Note that curvature is toward the axis for focusing phases; otherwise it is away.

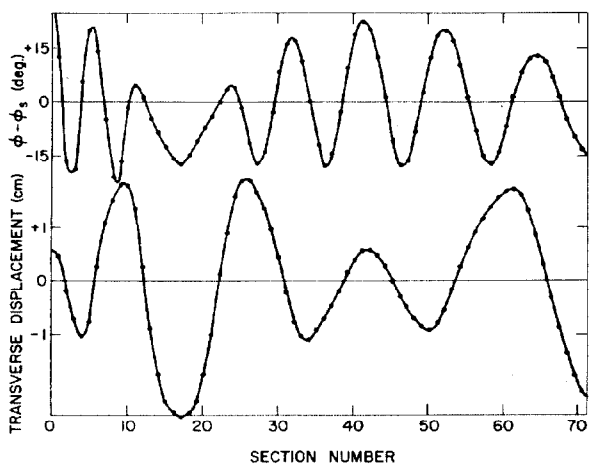


Fig. 3(b). Computer results for a transverse orbit coordinate and phase for lens strength in the neighborhood of  $\lambda_L = \lambda_R$ . Notice complementarity between amplitudes of radial and phase oscillations.

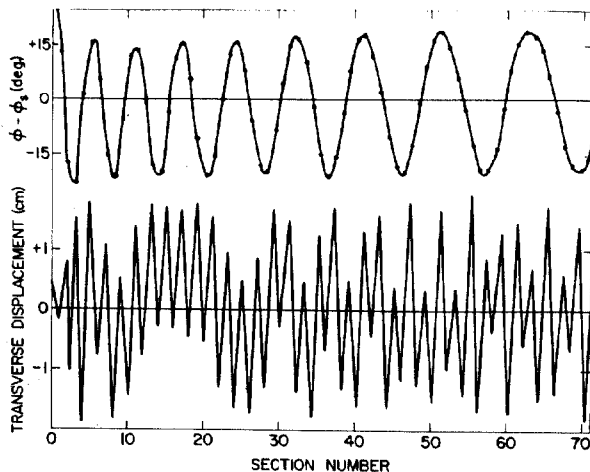


Fig. 3(c). Computer results for an orbit near the upper limit ( $\lambda_R = 2\lambda_L$ ) for lens strength.

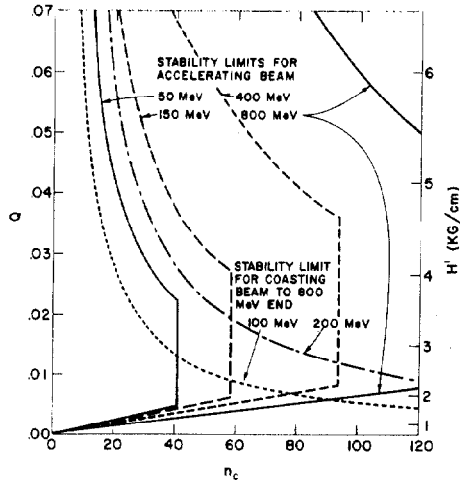


Fig. 4. Stable ranges for magnetic lens strength parameter. The right-hand ordinate is the field gradient for a doublet system with 10 cm magnets and 10 cm spacings/

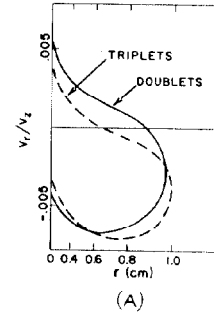


Fig. 5(a). Approximate radial acceptances for doublet and triplet systems to 800 Mev. Input is a monoenergetic 50 Mev proton beam with a  $90^\circ$  phase spread. Acceptance areas increase for smaller phase spreads and/or higher initial energies. Aperture radius = 2 cm.

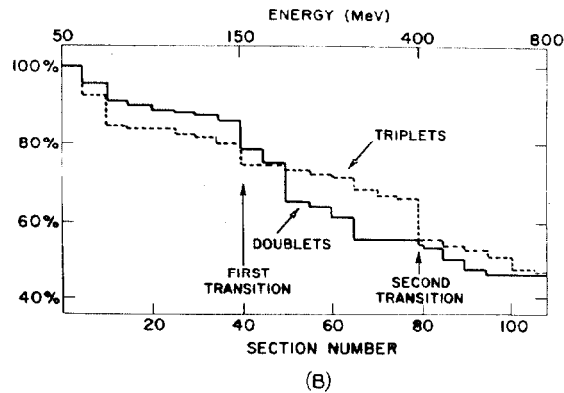


Fig. 5(b). Particle survival as a function of section number for typical computer runs with 150 particles. The jumps to longer sections are indicated by arrows. Note the differences in the ease with which the transitions are negotiated by the two systems, suggesting that some combinations may be optimum. The lens strength at the transition is taken to be the average of those appropriate to the two sides. Because of poor statistics, the differences in this and the preceding figure between triplets and doublets are probably not significant.